useful for the intensification of the mass transfer being conducted in the apparatus in a number of cases.

NOTATION

c, concentration of the diffusing impurity; D, its coefficient of diffusion; D_s, d_s, dimensional and dimensionless surface diffusion coefficients; g, acceleration of the external mass forces; J, j, dimensional and dimensionless diffusion flux density; h, film, thickness; L, L', linear scales; Q, q, fluid and surfactant substance discharge; u, velocity; U, V, dimensional and dimensionless surface velocities; x, y, y', longitudinal and transverse coordinates; α, β, perturbations of the homogeneous flow mode; Γ, γ, dimensional and dimensionless surfactant substance concentration; Δ, determinant in (24); δ, δ^*, quantities defined in (2) and (12); ζ, dimensionless film thickness; λ, quantity introduced in (11); μ, ν, dynamic and kinematic fluid viscosities; ξ, dimensionless longitudinal coordinate; ρ, fluid density; σ, coefficient of surface tension; the subscript zero refers to quantities in the initial section of the film, the asterisk subscript denotes quantities referring to the homogeneous flow mode.

LITERATURE CITED

1. L. E. Scriven and C. V. Sternling, Nature, 187, 186 (1960).
2. C. V. Sternling and L. E. Scriven, AIChE J., 5, 514 (1959).
3. S. P. Lin, AIChE J., 16, 375 (1970).
4. K. H. Wang, V. Ludviksson, and E. N. Lightfoot, AIChE J., 17, 1402 (1971).
5. L. M. Rabinovich, Prikl. Mekh. Tekh. Fiz., No. 2, 91 (1976).
6. E. Ruckenstein, Chem. Eng. Sci., 20, 853 (1965).
7. V. V. Dil'man, Yu. V. Aksel'rod, and F. M. Khutoryanskii, TOKhT, 11, 11 (1977).
8. V. Ludviksson and E. N. Lightfoot, AIChE J., 17, 1166 (1971).
9. W. J. Strobel and S. Whitaker, AIChE J., 15, 527 (1969).
10. S. K. Myasnikov, N. N. Kulov, V. A. Malyusov, and N. M. Zhavoronkov, TOKhT, 6, 893 (1972).
11. V. G. Levich and V. S. Krylov, in: Annual Review of Fluid Mechanics, Vol. 1, Palo Alto, Ca. (1969).
12. E. Ruckenstein, Int. J. Heat Mass Transfer, 11, 1753 (1968).

RHEOLOGY OF STRETCHING FOR POLYMER LIQUIDS

A. N. Prokunin and N. G. Proskurnina

UDC 532.5:532.135

Theoretical and experimental studies are presented on various effects in uniform isothermal stretching of elastic liquids.

This theoretical discussion of stretching is based on the rheological equations for an incompressible elastic fluid [1]; these equations give a close quantitative description of the behavior of such liquids under shear [2]. The minimum necessary number of rheological constants is four, and then the equations take the form:

$$\sigma' + p\delta = \eta s \exp\left(-\frac{\beta}{\mu} W_s\right) e + 2cW_1 - 2c^{-1}W_2; \quad (1)$$

$$c^{\nabla} - ce - ec + 2ce_p^* = 0; \quad c^{\nabla} = \dot{c} + \omega c - c\omega; \quad (2)$$

$$e_p^* = \frac{1}{2\mu\theta} \exp\left(-\frac{\beta}{\mu} W_s\right)\left[\left(c - \frac{I_1}{3}\delta\right) W_{s1} - \left(c^{-1} - \frac{I_2}{3}\delta\right) W_{s2}\right];$$

$$I_1 = \mathrm{Sp}\, c; \quad I_2 = \mathrm{Sp}\, c^{-1}; \quad 2\mu = \frac{\eta}{\theta}(1 - s); \quad (3)$$

$$2W_s = W(I_1, I_2) + W(I_2, I_1); \quad (4)$$

Institute of Problems of Mechanics, Academy of Sciences of the USSR, Moscow. Mendeleev Institute of Chemical Technology, Moscow.

Translated from Inzhenerno-Fizicheskii Zhurnal, Vol. 36, No. 1, pp. 42-50, January, 1979. Original article submitted December 26, 1977.

0022-0841/79/3601-0027$07.50

$$W_j = \frac{\partial W}{\partial I_j}; \quad W_{sj} = \frac{\partial W_s}{\partial I_j}; \quad \dot{\mathbf{c}} = \left(\frac{\partial}{\partial t} + v_\alpha \frac{\partial}{\partial x_\alpha}\right) \mathbf{c}.$$

Experiment has shown that the classical potential given by the theory of elasticity is applicable in the range of strains used for a polymer liquid:

$$W = \mu (I_1 - 3). \tag{5}$$

In that case,

$$W_1 = \mu; \quad W_2 = 0; \quad W_s = \frac{\mu}{2} (I_1 + I_2 - 6); \quad W_{s1} = W_{s2} = \frac{\mu}{2}. \tag{6}$$

We consider the homogeneous noninertial stretching of a cylindrical specimen; the kinematic matrices and invariants of the tensor c take the form

$$\mathbf{e} = \varkappa \begin{pmatrix} 1 & 0 & 0 \\ 0 & -1/2 & 0 \\ 0 & 0 & -1/2 \end{pmatrix}; \quad \boldsymbol{\omega} \equiv 0;$$

$$c = \begin{pmatrix} \lambda^2 & 0 & 0 \\ 0 & \lambda^{-1} & 0 \\ 0 & 0 & \lambda^{-1} \end{pmatrix}; \quad c^{-1} = \begin{pmatrix} \lambda^{-2} & 0 & 0 \\ 0 & \lambda & 0 \\ 0 & 0 & \lambda \end{pmatrix}; \tag{7}$$

$$I_1 = \mathrm{Sp}\, \mathbf{c} = \lambda^2 + 2\lambda^{-1}; \quad I_2 = \mathrm{Sp}\, \mathbf{c}^{-1} = 2\lambda + \lambda^{-2} \quad (\lambda \geqslant 1).$$

We substitute (5), (6), and (7) into (2) and (3) to get equations relating the elastic strain λ to the strain rate $\varkappa$:

$$\frac{1}{\lambda} \frac{d\lambda}{d\tau} + \frac{(\lambda + 1)(\lambda^3 - 1)}{6\lambda^2} \exp(-L) = \Gamma(\tau); \tag{8}$$

$$L = \frac{\beta}{2\lambda^2} (\lambda + 1)^2 (\lambda^2 - 4\lambda + 1) \quad (\tau = t/\theta; \ \Gamma = \varkappa\theta).$$

We substitute (5), (6), and (7) into (1) and use the condition that the radial components of the stress become zero at the surface of the cylindrical specimen to get the dimensionless tensile stress:

$$\sigma = \frac{\sigma'\theta}{\eta} = \frac{(\sigma'_{11} - p)\,\theta}{\eta} = (1 - s)(\lambda^2 - \lambda^{-1}) + 3s\Gamma \exp(L). \tag{9}$$

Equations (8) and (9) have been given in [3] for s = 0. The following is the rate of irreversible strain:

$$e_p^* = \frac{1}{6\theta} [\lambda^2 + \lambda - \lambda^{-1} - \lambda^{-2}] \exp(-L). \tag{10}$$

One-dimensional stretching (which can be performed in various ways in experiments) allows one to measure not only the stress σ and strain rate Γ but also the elastic recovery $\alpha = l/l_\tau$.*

We now consider the relationship between α and λ; Eq. (9) implies that the strain rate Γ during uniform contraction of a specimen on unloading is defined by

$$\Gamma = -\frac{(1 - s)}{3s} \frac{(\lambda^3 - 1)}{\lambda} \exp(-L) = \frac{d\varepsilon^*}{d\tau}. \tag{11}$$

Here $\varepsilon^* = \ln(l_\tau/l)$ (see [4]) and l_τ is the length of the specimen during contraction at time τ (at the start of contraction, $\tau = 0$, we have $l_\tau = l$; $l_\tau \to l_\Gamma$ for $\tau \to \infty$). It follows from (8) and (11) that during relaxation we have

$$\frac{d\lambda}{d\tau} = -\frac{(\lambda^3 - 1)}{3} \exp(-L) \left[\frac{\lambda + 1}{2\lambda} + \frac{1 - s}{s}\right]. \tag{12}$$

*The elastic-strain measures λ and α are equivalent in the theory of [1].

From (11) and (12) we have

$$\frac{d\varepsilon^*}{d\lambda} = \frac{2(1-s)}{\lambda(2-s)+s}.$$

The solution to this equation on the basis that $\varepsilon^* = 0$ and $\lambda = \lambda_0$ for $\tau = 0$ is:

$$\varepsilon^* = \frac{2(1-s)}{2-s} \ln \frac{s+\lambda(2-s)}{s+\lambda_0(2-s)}. \tag{13}$$

Formula (13) applies for any τ ($0 < \tau < \infty$), where τ is reckoned from the start of unloading; we pass to the limit $\tau \to \infty$ ($\lambda \to 1$, $l_\tau \to l_r$) in (13) to get equations relating α and λ_0 during stretching (here and subsequently we replace λ_0 by λ for simplicity):

$$\alpha = \left[\frac{s-\lambda(2-s)}{2}\right]^{\frac{2(1-s)}{2-s}}; \quad \lambda = \frac{2}{2-s}\alpha^{\frac{2-s}{2(1-s)}} - \frac{s}{2-s}. \tag{14}$$

Note that β is absent from (14), while the relation between λ and α is of power-law type for λ sufficiently large.

The rate of irreversible strain is determined by experiment as

$$e_p = \Gamma - \frac{d}{d\tau}\ln\alpha. \tag{15}$$

Then (12), (14), and (15) give

$$e_p = \Gamma\left(1 - \frac{\lambda}{\alpha}\frac{d\alpha}{d\lambda}\right) = \frac{\lambda}{\alpha}\frac{d\alpha}{d\lambda}\frac{(\lambda-1)(\lambda^3-1)}{6\lambda^2}\exp(-L). \tag{16}$$

Note that e_p and e_p^* in (10) are two measures of the rate of irreversible strain; the second is dependent only on λ, but e_p is additionally dependent on Γ. Further, $e_p = \sigma/3$ in the range of linear behavior of the liquid ($\ln\lambda \ll 1$) [4].

We now consider stretching with $\Gamma = \text{const}$; then (9) can be integrated. If τ is small, viz., $\Gamma\tau \ll 1$, we have $\lambda \approx e^{\Gamma\tau}$,† i.e., Voigt's nonlinear model can be used to describe the strain. The range in λ showing elastic behavior then increases with Γ. Steady-state flow is attained ($d\lambda/d\tau \equiv 0$) for $\beta = 0$ and for any Γ. The usual quantity determined by experiment is the dimensionless effective viscosity σ/Γ in steady-state flow ($\beta = 0$) and the value ranges from 3 to $6 - 3s$ as (8) shows.

If $\beta \neq 0$ [3], we derive the value Γ_{cr}, viz., the critical value for which no state of steady flow is attained, i.e., where $\sigma(\tau)/\Gamma$ and $\lambda(\tau)$ both increase with τ. Further, if $\beta < 10^{-2}$, we get that $\Gamma_{cr} = {}^1/_3 e\beta$, and (8) implies that $\lambda = e^{\Gamma\tau}$ for $\lambda \to \infty$.

Therefore, if $\Gamma > \Gamma_{cr} \gg 1$ and τ is large or small we have $\lambda \approx e^{\Gamma\tau}$ and (9) gives an approximate relationship for σ as

$$\sigma = (1-s)e^{2\Gamma\tau} - 3s\Gamma\exp\left(\frac{\beta}{2}e^{2\Gamma\tau}\right).$$

We computed the τ dependence of λ, σ, α, and e_p by means of (8), (9), (14), and (16), respectively. The results are compared with measures in what follows.

We used molten polyisobutylene type P-20 (molecular weight about 10^5), which differed somewhat from that used in [5, 6]. The maximum (Newtonian) viscosity of the polymer was $\eta \approx 1.1 \cdot 10^6$ Pa·sec. The equilibrium elastic modulus [4] was $G \approx 1.5 \cdot 10^3$ Pa. All the experiments were performed at 22°C.

Stretching with $\varkappa = \text{const}$ was performed either in a system in which the base length of the specimen was constant [5], in which case the stretching was performed with a single roller, or else with a variable-base system‡ [6]. Stress-relaxation measurements were also performed; in the latter case, the stretching was halted almost instantaneously and the stress as a function of time at a fixed length was then recorded.

The systems of [5, 6] gave strain rates between $3.84 \cdot 10^{-4}$ and 10^{-1} sec^{-1} and strains $\varepsilon = r_0^2/r^2$ up to 40 (r_0 and r are the radii of the specimen before deformation and at the

†Here e is the base of the natural logarithm.

‡This apparatus was built in the workshops of the Institute of Chemical Fibers, Academy of Sciences of the USSR.

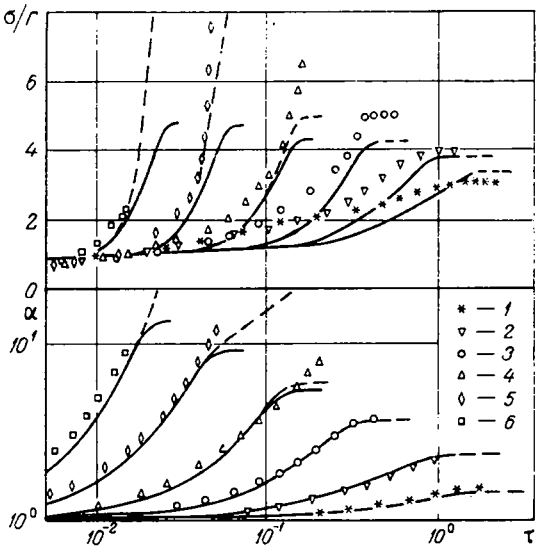

Fig. 1. Effects of time τ on: a) effective viscosity σ/Γ; b) elastic recovery α; the points are from experiment, while the solid lines are from theory: 1-6) Γ = 0.768, 2.4, 7.68, 24, 76.8, and 200, respectively.

time of deformation). The restrictions on $\varkappa$ and ε for the system of [6] were related to design features and to nonuniformities appearing in the specimens when the radius of the latter was small. The restrictions on ε for the system of [5] were related only to the nonuniformities. During stress relaxation (specimen theoretically immobile) the nonuniformity along the specimen may result in a certain amount of movement, particularly if the initial strain is large, and it is even possible for the specimen to fail during stretching and relaxation. The failure is evidently due to the differing time curves for the relaxation processes occurring for different initial states of strain.

The homogeneity of the specimens was always checked at least partially by photography at a fixed point.

The following τ curves were recorded: stretching force F, total strain ε (i.e., radius r and stress σ), and elastic recovery $\alpha = l/l_r$; here l_r is the length to which a section of length l in the stretched specimen tends when the external stress is eliminated (σ = 0), viz., the theoretical value for $t \to \infty$. In practice, the contraction of a piece of specimen of length l cut by means of knives was essentially complete within 1 h [4].

Certain further details of the measurements are given below in discussing the results. The spread taken over the entire set of data was fairly large, and it rose to ±15% for large strains.

Figure 1 shows the τ dependence of the effective viscosity $\sigma/\Gamma = \sigma'/\eta\varkappa$ and of α for various $\Gamma = \varkappa\theta$; here $\theta = 2 \cdot 10^3$ sec and $\eta = 1.1 \cdot 10^6$ Pa·sec. Steady-state yield was obtained for $\Gamma \leq 24$, and the curve drawn through the points 1 corresponds to linear behavior of the liquid. The effective viscosity σ/Γ and α increase with Γ in steady-state yield, as has been reported previously [6, 7]. The larger Γ, the smaller the τ at which this steady yield occurs. No steady state was reached for $\Gamma > 24$, but it is not known whether this is an inherent feature or merely a consequence of the above restrictions on ε.

Figure 2a shows the α dependence of the dimensional stress σ' (the constants of the liquid are shown in dimensional form in Fig. 2 for simplicity). The open symbols represent σ'(α) during stretching at various constant rates of strain. These curves are derived from the measurements of Fig. 1a and b. The last point for $\varkappa \leq 1.2 \cdot 10^{-2}$ sec^{-1} (the points with the largest α) corresponds to steady-state yield. The filled symbols in Fig. 2a represent the envelope. The method of deriving this is illustrated by Fig. 2b.

The points in Fig. 2b give σ'(α) for stress relaxation, while the points with arrows represent (σ', α) and are the points from which the relaxation was started. We now consider the derivation of the σ'(α) curves. During stress relaxation, the stress σ'(t) alters (the

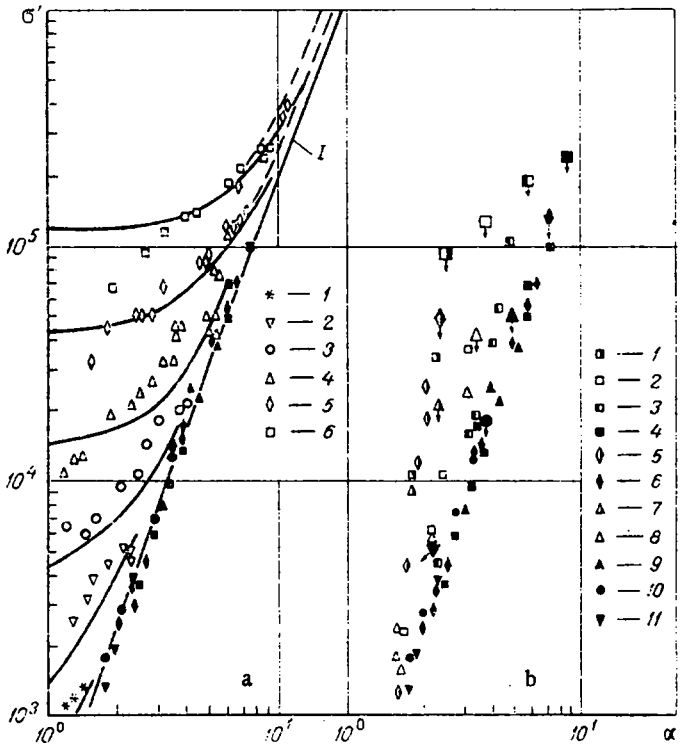

Fig. 2. The α dependence of σ' in Pa: a) for stretching (1-6): $\varkappa = 3.84 \cdot 10^{-4}$, $(1.2, 3.84) \cdot 10^{-3}$, $(1.2, 3.84) \cdot 10^{-2}$ and 10^{-1} sec^{-1}, where the filled symbols are the envelope values; b) during stress relaxation after stretching (1-4): $\varkappa = 10^{-1}$ sec^{-1} and $\ln \varepsilon = 1.3$, 1.8, 2.35 and 2.9; 5,6) $\varkappa = 3.84 \cdot 10^{-2}$ sec^{-1} and $\ln \varepsilon = 1.15$ and 2.9; 7-9) $\varkappa = 1.2 \cdot 10^{-2}$ sec^{-1}, $\ln \varepsilon = 1.30$, 2.16, 2.9; 10) $\varkappa = 3.84 \cdot 10^{-3}$ sec^{-1}, $\ln \varepsilon = 2.9$; 11) $\varkappa = 1.2 \cdot 10^{-3}$ sec^{-1}, $\ln \varepsilon = 2.6$.

specimen has previously been stretched), and for this purpose the specimen was cut up at various times t and the elastic recovery α was measured. Naturally, this interfered with the stress relaxation, and the experiment had to be repeated to yield the next value of α. This gave α(t) during stress relaxation. The α(t) and σ'(t) curves (not given here) were used to plot the σ'(α) curves of Fig. 2b.

Figure 2b shows that the σ'(α) data fit a single curve if the relaxation starts from (σ', α) points lying on that curve (e.g., points 3, 8, and 11). Note that ε is roughly the same for these points. The stresses during relaxation were produced by stretching specimens to various ϰ. All the curves of Fig. 2b converge to a single curve, which is the envelope for the various σ'(α) curves (the stretching and relaxation curves arise from this, as parts a and b of Fig. 2 show). Forthcoming papers will demonstrate that the envelope constructed in this way remains the same for other states of deformation. The envelope is attained most rapidly as α varies if one starts from the steady-state points on the stretching curve.

Figure 3 shows $e_p(\alpha) = \Gamma - [(d \ln \alpha)/d\tau]$ for various Γ; these curves were derived from the α(τ) derived during stretching with Γ = const (Fig. 1b). The $e_p(\alpha)$ curves resemble the σ(α) curves in having an envelope (filled symbols in Fig. 3). This envelope was derived by constructing the following curves (not given here):

$$e_p(\alpha) = -\frac{1}{\alpha}\frac{d\alpha}{d\tau}. \qquad (17)$$

Here α(τ) is the time dependence of the elastic recovery during relaxation (see above for the method of derivation). Formula (17) follows from the definition of e_p for $\Gamma \equiv 0$, and the curves given by (17) converge to a single curve (the envelope) during stress relaxation (Fig. 2b), as for σ(α). The curves of (17) attain the envelope most rapidly if the α(τ) curves are derived starting from the state of steady yield during stretching.

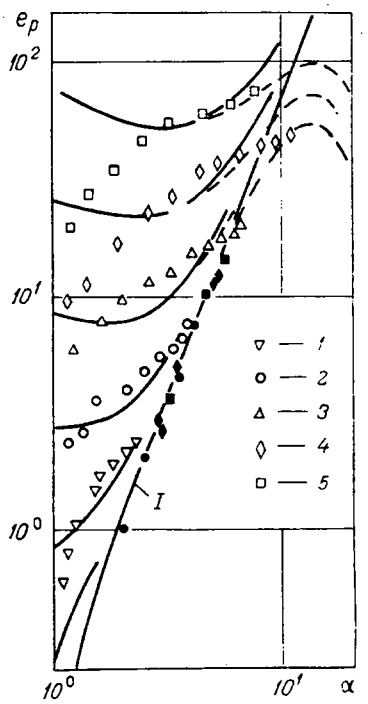

Fig. 3. The α dependence of the e_p of (15) for: 1-5) Γ = 2.4, 7.68, 24, 76.8, and 200.

We now compare the theoretical results with experiment. We start with the determination of the unknown constants η, s, and θ.

The viscosity η was taken as the maximum (Newtonian) viscosity as determined in the region of linear behavior from steady-state experiments on shear and stretching [4]. The values for the viscosity given by both methods were the same within the error of the experiments and were $\eta \approx 1.1 \cdot 10^6$ Pa·sec.

We determined s and θ by means of the envelope derived for $\sigma'(\alpha)$ from the stress-relaxation experiments (Fig. 2). The following dimensional form can be given for the theoretical envelope, as is clear from (9) with $\Gamma \equiv 0$:

$$\sigma_1' = \frac{\eta(1-s)}{\theta}(\lambda^2 - \lambda^{-1}). \tag{18}$$

Figure 2a shows the theoretical envelope denoted by I; we have from (14) and (17) that the following applies for λ sufficiently large:

$$\lambda \sim \alpha^{\frac{2-s}{2(1-s)}}; \quad \sigma_1' \sim \alpha^{\frac{2-s}{1-s}}. \tag{19}$$

and therefore (19) can be plotted in log–log coordinates to give a curve approximating closely to a straight line having the coefficient of proportionality $\approx 2.5 = (2 - s)/(1 - s)$, which gives $s = 0.35$.

As η is known (see above) and s has been determined, we merely specify that (19) must agree with experiment (see the filled symbols in Fig. 2a), and this gives $\theta = 2 \cdot 10^3$ sec.

A point here is that all the other theoretical curves given in this paper have been calculated from the θ and s derived solely from the observed envelope. Also, the relaxation time derived as $\eta/G \approx 0.8 \cdot 10^3$ sec is only half the θ derived from the envelope.

In accordance with (9), the observed relaxation curves (Fig. 2b) were approximated by means of an instantaneous jump of $3\eta s\varkappa \exp(L)$ from the point of onset of relaxation to the envelope, with the subsequent change occurring along the envelope as α decreased.

The classical potential of (5) from the theory of elasticity was used in deriving (18), and this is clearly appropriate.

Parts a and b of Fig. 1 (solid lines) show theoretical τ-dependence curves for σ/Γ and α as calculated from (8), (9), and (14) for $\beta = 0$; the main deficiency of the theoretical description is that $\sigma/\Gamma \leq 5.0$, whereas the experimental curves run up to values in excess of

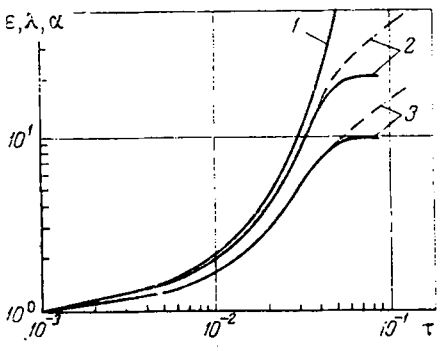

Fig. 4. Theoretical τ-dependence of: 1) total strain ε; 2) elastic strain λ; 3) elastic recovery α.

8. This was overcome by assuming $\beta = 1.72 \cdot 10^{-3}$, and a point here is that steady-state yield does not exist for $\Gamma = 76.8$.

Here and subsequently the solid lines correspond to $\beta = 0$, while the broken lines correspond to $\beta = 1.72 \cdot 10^{-3}$; if the theoretical results for the two cases are the same, only the solid line is given.

The theoretical curves of Fig. 2a have been derived from the theoretical $\sigma(\tau)$ of Fig. 1b together with (9) and (14).

The e_p of Fig. 3 were calculated from (16) for stretching; the theoretical envelope for e_p derived from this formula for $\Gamma \equiv 0$ takes the form

$$e_p^* = \frac{1}{\alpha} \frac{d\alpha}{d\lambda} \frac{(\lambda - 1)(\lambda^3 - 1)}{6\lambda^2} \exp(-L).$$

The envelope is dependent on β and is denoted by I in Fig. 3.

We now compare the theoretical relationships for $\varepsilon = e^{\Gamma\tau}$, $\lambda(\tau)$, and $\alpha(\tau)$; these curves are shown in Fig. 4 for $\Gamma = 76.8$. Note that $\lambda \approx \varepsilon$ for τ small, i.e., the medium deforms as a nonlinear Voigt solid, as (9) shows for $\lambda = \varepsilon$. Large elastic strains occur (e.g., $\lambda \approx \varepsilon \leqslant 10$ in Fig. 4). Note that the elastic recovery λ is less than the elastic strain λ ($\alpha \leqslant 5$ for $\lambda \approx \varepsilon = 10$ in Fig. 4).

These results show that the theoretical description deteriorates for all Γ as α decreases (the linear range of description). The description is improved somewhat for fairly large Γ and α by the introduction of β.

The strain occurring for τ small, when there is virtually no yield, shows that the failure observed, e.g., with monodisperse polymers [8] can be explained without the need to invoke a mechanism for the loss of fluidity ($\beta \neq 0$) [3].

The Voigt nonlinear model of (1)-(3) with $\beta = 0$ and $e_p^* = 0$ can thus be of value in solving many practical problems in the deformation of melts and concentrated solutions of polymers.

NOTATION

σ', stress tensor; p, isotropic pressure; δ, unit tensor; e, strain-rate tensor; c, elastic-strain tensor; I_1, I_2, major invariants; $W(I_1, I_2)$, elastic potential; e_p^*, tensor for irreversible-strain rate; ω, vortex tensor; β, dimensionless parameter characterizing elasticity of macromolecular chains ($0 \leq \beta \leq 1$); η, maximum (Newtonian) viscosity; θ, relaxation time; s, ratio of retardation time to relaxation time ($0 < s < 1$); t, τ, dimensional and dimensionless times; v_α, velocity components; x_α, Cartesian coordinates; ×, Γ, dimensional and dimensionless longitudinal strain rates; λ, α, measures of elastic strain; σ', σ, dimensional and dimensionless tensile stresses; l, sample length at instant τ; l_r, limit to l in stress relaxation ($\sigma \equiv 0$) for $\tau \to \infty$; ε, total longitudinal strain; r_0, r, initial and current sample radii; F, tensile force.

LITERATURE CITED

1. A. I. Leonov, Rheol. Acta, 15, No. 2 (1976).
2. A. I. Leonov, E. H. Lipkina, E. D. Paschin, and A. N. Prokunin, Rheol. Acta, 15, Nos. 7/8 (1976).
3. A. I. Leonov, É. Kh. Lipkina, and A. N. Prokunin, Zh. Prikl. Mat. Tekh. Fiz., No. 4, 86 (1976).

4. A. I. Leonov, A. N. Prokunin, and G. V. Vinogradov, in: Advances in Polymer Rheology [in Russian], Khimiya, Moscow (1970), p. 40.
5. M. S. Akutin, A. N. Prokunin, N. G. Proskurnina, and O. Yu. Sabsai, Mekh. Polim., 2, 353 (1977).
6. V. D. Fikhman, B. V. Radushkevich, and G. V. Vinogradov, in: Advances in Polymer Rheology [in Russian], Khimiya, Moscow (1970), p. 9.
7. H. M. Laun and H. Münstedt, Rheol. Acta, 15, No. 10 (1976).
8. V. V. Volosevich, "A study of the viscosity and limiting (failure) parameters of linear elastomers by uniaxial stretching," Candidate's Dissertation, Moscow Institute of Fine Chemical Technology, Moscow (1976).

HEAT EXCHANGE IN THE FLOW OF A SYSTEM OF AXISYMMETRIC LIQUID JETS ONTO A NORMALLY PLACED PLANE BARRIER

P. A. Pyass and A. A. Kiis

UDC 536.242:532.525.2

The influence of the geometrical and physical parameters of a system of axisymmetric jets impinging on a barrier on the heat-transfer coefficient and the final temperature of the liquid is analyzed.

The flow arising in the region of interaction of a turbulent jet with a barrier has a whole series of peculiarities. The pattern of motion is so complicated in details that a theoretical calculation of the boundary layer becomes very difficult [3]. It is therefore necessary to conduct experimental investigations.

A number of reports [1, 5, 6, 8, 9, 10] have been devoted to heat exchange in the interaction of single jets of dropping liquids with barriers, but there is an absence of investigations in which heat exchange in the interaction of a system of axisymmetric nonflooded jets of dropping liquid with a surface is analyzed, which might be used to design and build highly efficient liquid-jet heat exchangers. In the given case it should be noted that the average heat-transfer coefficient from a wall to a liquid depends on the velocity of the liquid, the geometrical characteristics of the system, and the thermophysical properties of the liquid:

$$\alpha = \varphi(w;\ d_e;\ f;\ F;\ \rho;\ \lambda;\ \nu;\ c_p). \tag{1}$$

Using dimensional analysis, in dimensionless form we find

$$\frac{\alpha d_e}{\lambda} = \varphi\left(\frac{\nu}{w d_e};\ \frac{\lambda}{\rho c_p \nu};\ \frac{f}{F}\right)$$

or

$$\mathrm{Nu} = \varphi(\mathrm{Re};\ \mathrm{Pr};\ A_f). \tag{2}$$

To obtain Eq. (2) in explicit form we constructed a model of a jet heat exchanger and carried out experimental investigations. The area of the heat-exchange surface of the apparatus was 0.0145 m^2, the number of nozzles in the perforated plate ranged from 33 to 121, and the dimensionless distance between the heat-exchange surface and the nozzles ranged from 50 to 100. The nozzle diameter was the same in all the tests and equalled 0.5 mm. Water was used as the liquid and moist steam from an industrial boiler served as the heat-transfer agent.

The final temperature of the falling liquid film was taken as the controlling temperature in the treatment of the test data. The height L of the heated plate was taken as the characteristic dimension in the Nusselt number. The Reynolds number was converted to the form $\mathrm{Re} = 4\Gamma/\rho\nu$.

Estonian Agricultural Academy, Tartu. Translated from Inzhenerno-Fizicheshkii Zhurnal, Vol. 36, No. 1, pp. 51-54, January, 1979. Original article submitted December 27, 1977.

 0022-0841/79/3601-0034$07.50